NATIONAL ADVISORY COMMITTEE FOR AERONAUTICS

TECHNICAL NOTE 3726

COMPRESSIVE AND TORSIONAL BUCKLING OF THIN-WALL CYLINDERS IN YIELD REGION

By George Gerard

New York University

Washington
August 1956

NATIONAL ADVISORY COMMITTEE FOR AERONAUTICS

TECHNICAL NOTE 3726

COMPRESSIVE AND TORSIONAL BUCKLING OF THIN-WALL CYLINDERS IN YIELD REGION

By George Gerard

SUMMARY

Based on assumptions which have led to the best agreement between theory and test data on inelastic buckling of flat plates, a general set of equilibrium differential equations for the plastic buckling of cylinders has been derived. These equations have been used to obtain solutions for the compressive and torsional buckling of long cylinders in the yield region.

Test data are presented which indicate satisfactory agreement with the theoretical plasticity-reduction factors in most cases. Where a difference in results exists, test data are in substantially better agreement with the results obtained by use of the maximum-shear law rather than the octahedral-shear law to transform axial stress-strain data to shear stress-strain data.

INTRODUCTION

Inelastic Compressive Buckling of Flat Plates

The state of knowledge up to 1936 concerning inelastic buckling of plates and shells has been summarized by Timoshenko in reference 1. The main efforts were concerned with attempts to modify the various bending-moment terms of the equilibrium differential equations by the use of suitable plasticity coefficients determined from experimental data on columns. Although such semiempirical efforts met with a reasonable degree of success, the theoretical determination of plasticity-reduction factors for flat plates has been achieved within recent years as the result of the development of inelastic-buckling theory. Because such developments are recent and form the background for the inelastic-buckling theory for shells developed herein, the following discussion concerning the assumptions and results of the various theories is presented in some detail.

Different investigators have used differing assumptions in the development of their theories. The major assumptions underlying each of these theories are given in the following table.

Investigator	Stress-strain law	Plasticity law	Buckling model
Bijlaard (ref. 2)	Incremental and deformation types, ν instantaneous	Octahedral shear	No strain reversal
Ilyushin (ref. 3)	Deformation type, $\nu = 0.5$	Octahedral shear	Strain reversal
Handelman and Prager (ref. 4)	Incremental type, ν instantaneous	Octahedral shear	Strain reversal
Stowell (refs. 5 and 6)	Deformation type, $\nu = 0.5$	Octahedral shear	No strain reversal

Historically, Bijlaard (ref. 2) appears to have been the first to arrive at satisfactory theoretical solutions for inelastic-buckling theories. His work is the most comprehensive of all those considered in that he considers both incremental and deformation theories and concludes that the deformation type is correct since it leads to lower inelastic buckling loads than those obtained from incremental theories. His work was first published in 1937. That paper and later publications include solutions to many important inelastic-buckling problems. However, this work appears to have remained unknown to most of the later investigators.

Ilyushin (ref. 3) briefly referred to Bijlaard's work and then proceeded to derive the basic differential equation for inelastic buckling of flat plates according to the strain-reversal model. The derivation of this equation is rather elegant and was used by Stowell (ref. 5), who, however, used the no-strain-reversal model. The differential equation obtained by Bijlaard reduces to that derived by Stowell by setting $\nu = 1/2$ in the former. Handelman and Prager (ref. 4), during this time, obtained solutions to several inelastic-buckling problems by use of incremental theory. Test data on compressed flanges and plates indicate that the results of incremental theories are definitely unconservative regardless of the buckling model, whereas deformation-type theories are in relatively good agreement.

The problem of plastic buckling has also been the subject of much experimental research. The use of the secant-modulus-reduction factor was first proposed for plates under compressive loads by Gerard (ref. 7) on the basis of tests on Z- and channel sections. Later, Stowell (ref. 5) proved theoretically that use of the secant modulus is correct for hinged flanges and that for elastically restrained flanges and plates the

plasticity-reduction factor includes a function of the tangent modulus in addition to the secant modulus. For long columns, the factor depends only upon the tangent modulus. The plasticity-reduction factors proposed by Stowell for simply supported flanges and plates have received excellent experimental confirmation (refs. 8 to 10) and it has been well known for some 50 years that the tangent modulus is in good agreement with test data for columns. Thus, the theoretical plastic-buckling factors for plates under compressive loads appear to be well substantiated by rather precise experimental data.

Inelastic Shear Buckling of Flat Plates

In contrast with plastic compressive buckling, shear buckling of plates appears to be on less substantial ground. As the result of a series of tests on long 2024-0 aluminum-alloy plates under shear, Gerard (ref. 11) proposed use of the shear secant modulus as the plasticity-reduction factor for this case. The shear secant modulus is determined from a shear stress-strain curve, which, according to reference 11, is to be derived from an axial stress-strain curve on the basis of the maximum-shear plasticity law. Stowell (ref. 6) derived a theoretical plasticity-reduction factor for shear which has virtually the same numerical value for all conditions of elastic restraint between simple support and clamped.

In comparing the test data of reference 11 with the theoretical reduction factor, Stowell used a shear stress-strain curve derived by the octahedral-shear plasticity law. The shear plastic-buckling test data were found to lie consistently below the theoretical factor. Furthermore, Stowell attempted to explain the agreement between the shear secant-modulus method proposed in reference 11 and the test data therein on the basis that the stress-strain curve for 2024-0 aluminum alloy can be well approximated by a power law.

Recently, in a series of tests on long, square, 2014-T6 aluminum-alloy tubes in torsion, Peters (ref. 10) presented a new set of test data on plastic shear buckling. Although the stress-strain curve of this material cannot be adequately approximated by a power law, excellent agreement was found to exist between the new test data and the shear secant-modulus method proposed in reference 11. The theoretical factors of Stowell (ref. 6) and Bijlaard (ref. 2) were found to be consistently higher than the test data by an order of approximately 15 percent in the buckling stress.

In summarization, then, the assumptions which lead to the best agreement between theory and test data on inelastic buckling of aluminum-alloy flat plates under compression loading are deformation-type stress-strain laws, stress and strain intensities defined by the octahedral-shear law,

and the no-strain-reversal model of inelastic buckling. Although there may be theoretical objections to deformation theories as a class and the use of a no-strain-reversal model in conjunction with classical stability concepts, test data do suggest the use of results obtained from a theory based on these assumptions.

For the inelastic buckling of flat plates under shear loading, plastic-buckling theory and the test data are not in good agreement. The principal difficulty appears to lie in the use of the octahedral-shear law to transform stress-strain data under axial loading to shear stress-strain data. This situation is discussed further herein in connection with results obtained for torsional buckling of cylinders.

Inelastic Buckling of Cylinders

Timoshenko (ref. 1) has presented some attempts to describe the inelastic buckling of a cylinder under axial compressive forces subjected to axisymmetric buckling. These results are based on the intuitive use of the reduced modulus in place of the elastic modulus where the latter appears in the elastic-buckling-stress equation.

Bijlaard (ref. 12), in an extension of his theory for inelastic buckling of flat plates, has considered the inelastic buckling of a cylinder subject to compression. Both the axisymmetric and the circumferential modes of buckling were considered in this analysis. The results are discussed in subsequent sections of this report.

In this paper, a general set of equilibrium differential equations for the plastic buckling of cylinders is derived. This set of equations is perfectly general and applies to any loading system leading to buckling. In particular, solutions are obtained for compressive and torsional buckling of long cylinders in the yield region.

The plasticity terms appearing in the equilibrium equations depend upon the choice of the buckling model. For the no-strain-reversal model, which is used in this analysis, the fact that the axial load must increase slightly during buckling in order that no unloading should occur presents a mathematical difficulty when using classical stability concepts in which the loading remains constant during buckling. This difficulty is discussed and an attempt to remove it is presented.

This investigation was conducted at New York University under the sponsorship and with the financial assistance of the National Advisory Committee for Aeronautics.

SYMBOLS

A_i	plasticity coefficients defined by equations (A13)
B	axial rigidity, $E_s t/(1 - \nu^2)$
b	plate width
D	bending rigidity, $E_s t^3/12(1 - \nu^2)$
d	diameter
E	modulus of elasticity
E_s	secant modulus
E_t	tangent modulus
e_i	strain intensity defined by equation (A2)
F_x, F_θ, F_z	force
G	shear elastic modulus
G_s	shear secant modulus
k_s	shear buckling coefficient
l	length of cylinder
M	bending moment per unit width
m	number of longitudinal half wave lengths
N	loading per unit width
n	number of circumferential wave lengths
p	external pressure
R	radius of cylinder
t	thickness

u,v,w displacements

x,θ,z coordinates

$\alpha = \left(3/\sigma_i^2\right)\left[1 - \left(E_t/E_s\right)\right]$

$\beta = t^2/12R^2$

γ shear strain

ϵ axial strain

η plasticity-reduction factor

$\lambda = l/m$

ν Poisson's ratio

ν_e elastic value of Poisson's ratio, equal to 0.3

σ axial stress

σ_i stress intensity defined by equation (A1)

τ shear stress

$\varphi = \tau_{cr}\left(1 - \nu^2\right)/E_s$

χ curvature

∇^4 operator, $\left[\left(\partial^2/\partial x^2\right) + \left(\partial^2/R^2\partial\theta^2\right)\right]^2$

$\nabla^8 = \left(\nabla^4\right)^2$

$( )'$ variations which arise during buckling, such as M' and N'

Subscripts:

c compression

cr critical

e elastic

f	failing
s	shear
x,y,xy	coordinate orientation for M, N, σ, and ϵ
1,2,3	variations which arise during buckling in ϵ and χ

EQUILIBRIUM EQUATIONS

The plan followed in this report is to present the theoretical derivations in appendixes. The theoretical results, comparisons with test data, and a discussion of the significance of these results appear in the main body of the report.

In appendix A, the assumptions of the plasticity theory used are discussed and the stress and strain intensities are defined according to the octahedral-shear law. Considerations involved in the buckling model are then considered and the incremental forces and moments which arise during buckling are presented based on the no-strain-reversal model.

In appendix B, Donnell's (ref. 13) simplified strain-displacement and equilibrium equations derived originally for cylinder elastic-buckling problems are combined with the incremental force and moment relations of appendix A. In this manner, a complete set of equilibrium differential equations is obtained for use in the solution of cylinder plastic-buckling problems. Included in appendix B is an attempt to remove the difficulty of using equilibrium equations based on classical stability concepts for inelastic-buckling problems in which the no-strain-reversal model requires that the load must increase slightly during buckling.

AXIAL COMPRESSIVE BUCKLING OF A LONG CYLINDER

Solution of Problem

In appendix C, the axisymmetric buckling of a long cylinder under axial compression is considered. The critical stress obtained by use of the equilibrium equations derived in appendix B has the following form:

$$\sigma_{cr} = \left[3\left(1 - \nu^2\right)\right]^{-1/2} E_s \left(E_t/E_s\right)^{1/2} t/R \qquad (1)$$

As in the inelastic buckling of flat plates, all effects of exceeding the proportional limit are incorporated in a plasticity-reduction factor defined as follows:

$$\eta_c = \sigma_{cr} \Big/ (\sigma_{cr})_e \tag{2}$$

The solution for the elastic case is obtained by substituting $E_s = E$, $E_t/E_s = 1$, and $\nu = \nu_e$ in equation (1):

$$(\sigma_{cr})_e = \left[3\left(1 - \nu_e^2\right)\right]^{-1/2} Et/R = 0.6Et/R \tag{3}$$

By use of equation (2),

$$\eta_c = \left(\frac{1 - \nu_e^2}{1 - \nu^2}\right)^{1/2} \frac{E_s}{E}\left(\frac{E_t}{E_s}\right)^{1/2} \tag{4}$$

In general, therefore,

$$\sigma_{cr} = 0.6\eta_c E(t/R) \tag{5}$$

Bijlaard (ref. 12) has previously obtained results equivalent to equations (1) and (4). His results are more exact, in fact, since the variation of Poisson's ratio in the inelastic range is included directly in the analysis. In the interests of simplicity, the present analysis utilizes the artificial device of taking $\nu = 1/2$ in both the elastic and plastic regions and then employs an approximate correction (see eq. (C15)) which yields exact solutions for the elastic and plastic ranges as limits. This method follows a suggestion of Stowell (ref. 5).

The purpose here in obtaining this solution was to present a unified approach to the compressive and torsional buckling of cylinders from the set of equilibrium equations derived in appendix B. Furthermore, equations (1) and (4) serve as a basis for interpreting test data presented herein on the inelastic buckling of cylinders.

In addition to the axisymmetric case considered here, Bijlaard (ref. 12) has also considered the circumferential buckling mode of a cylinder under axial compression. As in the elastic case, the critical stresses obtained for both buckling modes are essentially the same. Bijlaard has pointed out that for mild steel the circumferential mode may lead to a slightly higher buckling load than the axisymmetric mode.

It would be a relatively simple matter to solve the circumferential buckling case by use of the equilibrium equations of appendix B. However, in view of Bijlaard's results and the fact that the axisymmetric mode is often observed in tests on round cylinders which buckle plastically, the solution for this buckling mode was not pursued.

Test Data

Osgood (ref. 14) and Moore and Holt (ref. 15) have presented test data on the failing strength of drawn circular tubes under axial compression. Osgood tested 2017-T4 aluminum-alloy tubes for which compressive stress-strain curves were given and also chrome-molybdenum tubes for which, unfortunately, neither the compressive stress-strain curves nor compressive yield stresses were obtained. It is interesting to note that photographs of the test specimens indicate the appearance of axisymmetric buckling in some cases. Moore and Holt tested 6061-T6 aluminum-alloy tubes for which the compressive yield stresses were given although not the compressive stress-strain curves. A typical compressive stress-strain curve for this material, with a corresponding yield stress, was taken from reference 16 for correlation purposes.

To reduce the experimental data for comparison with theory, the experimental failing strength was divided by the critical elastic stress (eq. (3)) to determine the experimental plasticity-reduction factors given in table 1. The theoretical value of η_c was determined in each case by use of the pertinent stress-strain data according to equation (4). For Poisson's ratio, the following values were used:

$$\nu_e = 0.3 \tag{6}$$

$$\nu = 0.5 - \left(E_s/E\right)\left(0.5 - \nu_e\right)$$

The relation for the variation in Poisson's ratio in the yield region has been shown to apply to isotropic, plastically incompressible solids by Gerard and Wildhorn (ref. 17).

The theoretical and experimental values of η_c as a function of the inelastic-compressive-buckling stress are plotted in figure 1. For the limited range of test data on 2017-T4 and 6061-T6 aluminum-alloy tubes it can be observed that good agreement is obtained. This is remarkable in view of the fact that while it tends to confirm the relation for the plasticity-reduction factor (eq. (4)) it also confirms the classical small-deflection stability theory for compressed cylinders.

TORSIONAL BUCKLING OF A LONG CYLINDER

Cylinders of Extreme Length

In appendix D, the torsional buckling of a long cylinder is considered. If the cylinder is of sufficient length, the boundary conditions at the ends have negligible influence and two-lobe buckling occurs. The critical stress for this case obtained by use of the equilibrium equations of appendix B has the following form:

$$\tau_{cr} = 0.272\left(1 - \nu^2\right)^{-3/4} E_s(t/R)^{3/2} \tag{7}$$

In the elastic case, equation (7) becomes

$$\left(\tau_{cr}\right)_e = 0.272\left(1 - \nu_e^2\right)^{-3/4} E(t/R)^{3/2} \tag{8}$$

Donnell (ref. 13) has shown that equation (8) applies for

$$\left(\frac{l}{R}\right)^2\left(\frac{t}{R}\right) > a \tag{9}$$

where $a = 42$ for simply supported ends and $a = 60$ for clamped ends. By use of the equivalent of equation (2) for the torsional buckling case

$$\eta_s = \left(\frac{1 - \nu_e^2}{1 - \nu^2}\right)^{3/4} E_s/E \tag{10}$$

In general, therefore,

$$\tau_{cr} = 0.272\left(1 - \nu_e^2\right)^{-3/4} \eta_s E(t/R)^{3/2} \tag{11}$$

The plasticity-reduction factor depends primarily upon the secant modulus, which has been found to be the case whenever buckling occurs as a twisting action. This has been previously observed for compressive buckling of hinged flanges where buckling occurs as a twisting action and the plasticity-reduction factor depends primarily upon the secant modulus.

In appendix A, the secant modulus is defined as

$$E_s = \sigma_i / e_i \tag{12}$$

If the shear stress-strain curve is known (this can be relatively simply obtained by torsion tests on tubes although no such direct experimental procedure exists for obtaining these data for flat plates), then the respective stress and strain intensities according to equations (A1) and (A2) are as follows:

$$\sigma_i = (3)^{1/2}\tau \tag{13}$$

$$e_i = (3)^{-1/2}\gamma \tag{14}$$

By use of equation (12)

$$E_s = 3\tau/\gamma \tag{15}$$

Since $\tau/\gamma = G_s$, from equation (15)

$$G_s = E_s/3 \tag{16}$$

Therefore, equation (10) can be interpreted as

$$\eta_s = \left(\frac{1 - \nu_e^2}{1 - \nu^2}\right)^{3/4} G_s/G \tag{17}$$

in cases in which the shear stress-strain curve is available.

If, on the other hand, shear stress-strain data may not be available, then it is possible to construct a shear stress-strain curve from simple tension and compression stress-strain data by use of either the octahedral- or the maximum-shear law. As indicated in reference 11 for materials which are anisotropic as a result of straightening (Bauschinger effect), it is probably best to utilize an axial stress-strain curve which is an average of the tension and compression curves each at 45° with the direction of the applied shear. If the axial stress in the simple axial test is σ_x, then the stress and strain intensities according to the octahedral-shear and maximum-shear laws are

$$\left.\begin{aligned} \sigma_i &= \sigma_x \\ e_i &= \epsilon_x \end{aligned}\right\} \tag{18}$$

Thus, in both cases,

$$E_s = \sigma_x/\epsilon_x \tag{19}$$

However, the shear stresses corresponding to σ_x are different.

For octahedral shear

$$\tau = (3)^{-1/2}\sigma_x \tag{20}$$

and for maximum shear

$$\tau = \sigma_x/2 \tag{21}$$

Thus, the values of E_s and therefore η_s for a given value of σ_x correspond to a lower value of τ for the maximum-shear law as compared with that of the octahedral-shear law.

Cylinders of Moderate Length

A solution for the inelastic buckling of cylinders of moderate length, in which case the boundary conditions have a decided influence upon the buckling stress, has not been obtained herein. However, the elastic solution is known and has been given in the following form by Batdorf (ref. 18):

$$\tau_{cr} = 0.747E(t/R)^{5/4}(R/l)^{1/2} \tag{22}$$

for $50t/R < (l/R)^2 < 10R/t$.

For short cylinders defined approximately by $l^2/Rt < 1$, the flat-plate solution

$$\tau_{cr} = \frac{\pi^2 k_s \eta_s E}{12\left(1 - \nu_e^2\right)}\left(\frac{t}{b}\right)^2 \tag{23}$$

applies where

$$\eta_s = G_s/G \tag{24}$$

The plasticity-reduction factor for this case has been proposed by Gerard (ref. 11) and is based on the maximum-shear law to transform the axial stress-strain data to shear data.

Since equation (24) for short cylinders depends primarily upon the secant modulus as does equation (10) or (17) for long cylinders, it appears that equation (10) or (17) may be used as a reasonable approximation of η_s for cylinders of moderate length.

Test Data

Stang, Ramberg, and Back (ref. 19), Moore and Paul (ref. 20), and Moore and Holt (ref. 15) have presented test data on the torsional failing strength of long and moderate-length drawn circular tubes. In most cases failure occurred as a result of inelastic buckling in the two-lobe mode.

Stang, Ramberg, and Back tested 2017-T4 and chrome-molybdenum tubes for which representative shear stress-strain curves were presented. In this case, therefore, it was possible to correlate theory and experiment on the basis of equation (17). Of the large mass of test data given in reference 19, a relatively small amount was useful for correlation purposes. These data are given in table 2 and were selected on the basis that the tubes were long in the sense of equation (9) (clamped ends). Furthermore, the yield stress of the 2017-T4 tubes was approximately 23 ksi and the failing stress was less than 26 ksi to correspond with the given shear stress-strain data. For the chrome-molybdenum tubes, the corresponding values were 49 and 58 ksi, respectively. Many of the other test data were beyond the range of the given stress-strain data.

In computing the experimental values of η_s, the torsional failing stress was divided by the critical elastic shear stress of equation (8). Since the shear stress-strain data were given, the theoretical values of η_s were calculated by use of equations (17) and (6) for Poisson's ratio with G_s/G replacing E_s/E in the latter.

The theoretical and experimental values of η_s are shown in figure 2. It can be observed that good agreement is obtained for the 2017-T4 data, whereas the agreement is not so good for the chrome-molybdenum-tube data.

Moore and Paul (ref. 20) tested 6051-T6 seamless tubes of moderate length. Tension stress-strain data are also given. The torsional failing stresses are listed in table 3 together with the experimental value of η_s calculated by use of equation (22) for tubes of moderate length. The theoretical values of η_s were determined by use of equations (10) and (6), using the tension stress-strain data. Shown in figure 3 is a comparison of the η_s values based on the use of the octahedral- and maximum-shear laws to transform the axial stress-strain data. Better correlation is obtained with the latter, although the test data are below the theoretical values of η_s. This may possibly reflect the relatively large scatter among the test data or the fact that the value of η_s given by equation (10) is approximate for tubes of moderate length.

Relatively large scatter can also be observed for the 6061-T6 aluminum-alloy test data of Moore and Holt (ref. 15; also listed in table 3 and shown in fig. 3). These tests were conducted on both long tubes and tubes of moderate length and are so designated in table 3 and figure 3. The theoretical values of η_s were computed from a typical stress-strain curve for 6061-T6 aluminum alloy given in reference 16 and having the same yield properties as listed in reference 15. In this case, the test data again favor the use of the maximum-shear law to transform the axial data with approximately equal scatter of the test points about the theoretical line.

DISCUSSION

In discussing the correlation between the theoretical plasticity-reduction factors and the available test data, it is convenient to summarize the results as shown in table 4.

Compressive Buckling

For the limited amount of test data on 2017-T4 and 6061-T6 aluminum-alloy tubes in compression, it appears that the plasticity-reduction factor given by equation (4) is in substantially good agreement with test data. Considerably more weight must be placed on the 2017-T4 data as compared with the 6061-T6 data since compression stress-strain data were given for the former, whereas such data for the latter were estimated from other sources. Thus, the agreement obtained for the 2017-T4 data can be interpreted as excellent support for the theoretical value of η_c.

As indicated previously, the experimental values of η_c for the test data were computed using equation (3) which is based on classical

stability concepts. Since test data on elastic buckling of compressed cylinders generally fall considerably below this theoretical value, it appears fruitful to discuss the implications of the apparent agreement of test data on cylinders which buckle inelastically with equation (3) after inelastic buckling effects have been accounted for by use of η_c.

The cylinders used for the inelastic tests were drawn seamless tubes with R/t values less than 50. Consequently, these tubes probably contained very small geometrical imperfections and were relatively free of residual stresses. By contrast, tests on elastic buckling were generally conducted on cylinders fabricated from flat sheets with R/t values ranging from 200 to 3,000. Many of these tests were conducted on cylinders of very thin sheet stock and therefore the geometrical imperfections would be expected to be very much greater than those in drawn tubes. Thus, it is probably safe to conclude that the initial imperfections for the inelastic cylinders were considerably less than those for the elastic cylinders. Provided the plasticity-reduction factor is correct, the initial imperfections were apparently of such a small magnitude for the inelastic cylinders that the buckling stress is adequately predicted by classical small-deflection theory.

This apparent agreement with classical theory for inelastic cylinders may have some bearing on the currently held views concerning the lack of agreement of test data on elastic cylinders with small-deflection theory.

According to the energy criterion of buckling used by Tsien (ref. 21) for perfect elastic cylinders in a rigid screw-powered testing machine (the condition leading to the highest buckling stress)

$$\sigma_{cr} = 0.37Et/R \tag{25}$$

It is the contention of this theory that the small amount of energy necessary to trigger the jump to large deflections is available in the vibrations of the testing machine, for example.

Donnell and Wan (ref. 22) have maintained that the presence of geometrical imperfections and residual stresses rounds off the sharp peak in the stress end-shortening curve of large-deflection theory and therefore failure is observed at loads considerably below the classical value.

It is essential to realize that the highest buckling stress of the energy criterion is given by equation (25) and therefore this theory does not admit the possible realization of a buckling stress as high as that given by equation (3). On the other hand, as the imperfections become very small, equation (3) is approached as a limit in Donnell's interpretation. Since equation (3) was apparently confirmed by the test data

shown in figure 1, for which the imperfections were probably very small, it would appear that Donnell's interpretation is definitely favored over the energy criterion in this case.

Torsional Buckling

Of the test data available to evaluate the theoretical plasticity-reduction factor for torsional buckling given in figures 2 and 3 and summarized in table 4, it would appear that considerable weight should be placed on the 2017-T4 data. This is due to the fact that a wide range of test data as well as shear stress-strain data was given. For the chrome-molybdenum tubes only a small amount of test data could be used because the yield stresses and stress-strain properties varied considerably from those of the shear stress-strain curve given. Therefore, it would appear that excellent confirmation of η_s was obtained for the 2017-T4 data, whereas the chrome-molybdenum data were too few and too variable in stress-strain characteristics to permit any definite conclusions to be drawn for this material.

The 6051-T6 and 6061-T6 data of figure 3 are useful in providing a means of checking the theoretical value of η_s utilizing the maximum-shear and octahedral-shear laws to transform the axial stress-strain data to shear stress-strain data. Although the conclusions to be drawn are handicapped by relatively wide scatter of test data and by the nature of the stress-strain data available for correlation (table 4), it would appear that the data are in better agreement with the use of the maximum-shear law than with that of the octahedral-shear law to transform the axial data.

SUMMARY OF RESULTS

The following conclusions were derived from a theoretical and experimental investigation of the compressive and torsional buckling of thin-wall cylinders in the yield region:

1. A general set of equilibrium differential equations for plastic buckling of circular cylinders has been derived based on deformation stress-strain relations and the no-strain-reversal buckling model. Furthermore, an attempt has been made to remove a difficulty associated with using the no-strain-reversal model in conjunction with classical stability concepts.

2. The plasticity-reduction factors for inelastic buckling of long cylinders under compressive or torsional loadings have been derived.

It is shown that these factors are in satisfactory agreement with test data when satisfactory compression and shear stress-strain data are available.

3. Both the maximum-shear and octahedral-shear plasticity laws were used in transforming axial stress-strain data to shear stress-strain data for torsional buckling of cylinders in conjunction with a theoretically derived plasticity-reduction factor based on the octahedral-shear law. In such cases, results obtained by use of the transformed shear data based on the maximum-shear law are in better agreement with test data than those based on the use of the octahedral-shear law.

4. Compression test data on tubes which probably contained small geometrical imperfections correlated very well with the critical stress predicted by classical small-deflection theory after the theoretical correction for inelastic buckling had been incorporated. This correlation is viewed as a factor favoring the imperfection interpretation (Donnell) of tests on elastic cylinders over the energy interpretation (Tsien).

Research Division, College of Engineering,
New York University,
New York, N. Y., October 14, 1954.

APPENDIX A

PLASTICITY CONSIDERATIONS

In the following derivations, assumptions have been employed which appear to have resulted in the best agreement between theory and test data on inelastic buckling of flat plates with various geometrical boundary conditions and types of loading.

A fundamental hypothesis of plasticity theory is that the stress intensity σ_i is a uniquely defined, single-valued function of the strain intensity e_i for a given material when the stress intensity increases (loading) and is elastic when it decreases (unloading). The definitions of the stress and strain intensities theoretically can be chosen from a manifold of rotationally invariant functions. Two such functions, the maximum-shear and octahedral-shear laws, have been useful.

For the octahedral-shear law, the stress and strain intensities can be defined as follows:

$$\sigma_i = \left(\sigma_x^2 + \sigma_y^2 - \sigma_x\sigma_y + 3\tau^2\right)^{1/2} \tag{A1}$$

$$e_i = \frac{2}{\sqrt{3}}\left[\epsilon_x^2 + \epsilon_y^2 + \epsilon_x\epsilon_y + \left(\gamma^2/4\right)\right]^{1/2} \tag{A2}$$

With the assumption that the principal axes of stress and strain coincide, the secant modulus can be defined as

$$E_s = \sigma_i/e_i \tag{A3}$$

Furthermore, by use of deformation-type stress-strain laws together with the assumption of plastic isotropy and the idealization that Poisson's ratio is equal to 1/2 for both the elastic and the plastic region, the following simplified two-dimensional stress-strain laws are obtained:

$$\epsilon_x = \frac{1}{E_s}\left[\sigma_x - (1/2)\sigma_y\right] \tag{A4}$$

$$\epsilon_y = \frac{1}{E_s}\left[\sigma_y - (1/2)\sigma_x\right] \tag{A5}$$

$$\gamma = 3\tau/E_s \tag{A6}$$

Inelastic-Buckling Considerations

All of the foregoing assumptions form the basis for solution of plasticity problems in general. For the specific problem of inelastic buckling, it is necessary to make an additional assumption concerning the stress distribution at the instant of buckling.

From the standpoint of classical stability theory, the equilibrium differential equations are formulated on the basis that at the buckling load an exchange of stable equilibrium configuration occurs between the straight form and the slightly bent form. Since the load remains constant during this exchange, a strain reversal must occur on the convex side, and, therefore, the buckling model leading to the reduced-modulus concept for columns is correct theoretically.

Practical columns and plates invariably contain initial imperfections and therefore axial loading and bending proceed simultaneously. Since in the presence of relatively large axial compressive stresses the bending stresses are generally small, no strain reversal would be expected to occur and the incremental bending stresses in the inelastic range are given by the tangent-modulus model. However, the bent form is the only stable configuration in this case and therefore use of equilibrium equations based on perfect columns, plates, or shells is clearly unjustified.

Partially to remove this difficulty, Stowell has assumed that the straight form of the plate or column is stable until buckling occurs (ref. 5). At buckling, infinitesimal bending is assumed to proceed simultaneously with a corresponding infinitesimal increase in axial loading so that the plate is not subjected to a strain reversal and remains inelastic. Again this model poses an essential difficulty since classical stability theory is based on the assumption that the axial loading remains constant during the buckling process.

In appendix B, in which the equilibrium equations are considered, an attempt is made to remove this difficulty by showing that the infinitesimal increase in load associated with the no-strain-reversal model contributes higher order terms than those generally considered in the equilibrium equation. This is by virtue of the fact that the axial loads are multiplied by first or second derivatives of the displacements and

therefore products of the incremental load increase and these derivatives result in second-order terms.

Incremental Forces and Moments

When buckling occurs, the displacements vary slightly from their values before buckling. The resulting strain variations arise partly from variations of middle-surface strains and partly because of bending strains. These resulting variations of stresses have been considered by Ilyushin (ref. 3) and Stowell (ref. 5). Using the assumption that no part of the plate is unloaded, Stowell has derived the variations of the moments during the buckling process. The variations of the middle-surface forces can be derived directly from this work.

When the variations of the forces and moments are denoted by primes ('), the following relations apply to fully plastic plates during buckling:

$$N_x' = B\left[A_1\epsilon_1 + (1/2)A_{12}\epsilon_2 - (1/2)A_{13}\epsilon_3\right] \tag{A7}$$

$$N_y' = B\left[A_2\epsilon_2 + (1/2)A_{21}\epsilon_1 - (1/2)A_{23}\epsilon_3\right] \tag{A8}$$

$$N_{xy}' = \frac{B}{2}\left[A_3\epsilon_3 - (1/2)A_{31}\epsilon_1 - (1/2)A_{32}\epsilon_2\right] \tag{A9}$$

$$M_x' = -D\left[A_1\chi_1 + (1/2)A_{12}\chi_2 - (1/2)A_{13}\chi_3\right] \tag{A10}$$

$$M_y' = -D\left[A_2\chi_2 + (1/2)A_{21}\chi_1 - (1/2)A_{23}\chi_3\right] \tag{A11}$$

$$M_{xy}' = -\frac{D}{2}\left[A_3\chi_3 - (1/2)A_{31}\chi_1 - (1/2)A_{32}\chi_2\right] \tag{A12}$$

In equations (A7) to (A12), ϵ_1 and ϵ_2 are middle-surface normal strain variations and ϵ_3 is the middle-surface shear strain variation; χ_1 and χ_2 are the changes in curvature and χ_3 is the change in twist. Furthermore, the plasticity coefficients are defined as follows:

$$\left.\begin{aligned} A_1 &= 1 - \left(\alpha\sigma_x^2/4\right) \\ A_2 &= 1 - \left(\alpha\sigma_y^2/4\right) \\ A_3 &= 1 - \alpha\tau^2 \end{aligned}\right\} \tag{A13}$$

$$A_{21} = A_{12} = 1 - \left(\alpha\sigma_x\sigma_y/2\right)$$

$$A_{31} = A_{13} = \alpha\sigma_x\tau$$

$$A_{32} = A_{23} = \alpha\sigma_y\tau$$

where

$$\alpha = \left(3/\sigma_i^2\right)\left[1 - \left(E_t/E_s\right)\right]$$

The axial rigidity is

$$B = 4E_s t/3 \tag{A14}$$

The bending rigidity is

$$D = E_s t^3/9 \tag{A15}$$

In the elastic region, $\alpha = 0$ and, therefore, $A_1 = A_2 = A_3 = A_{12} = 1$ and $A_{13} = A_{23} = 0$. By replacing the definitions of equations (A14) and (A15) which are for a fully plastic plate by $B = Et/\left(1 - \nu_e^2\right)$ and $D = Et^3/12\left(1 - \nu_e^2\right)$, respectively, and replacing the coefficient (1/2) by ν_e, equations (A7) to (A12) reduce to the familiar relations for the elastic plate.

APPENDIX B

EQUILIBRIUM CONSIDERATIONS

Elastic Buckling

Donnell's equations (refs. 13 and 18) for elastic buckling of thin-wall circular cylinders have been used with a considerable degree of success in buckling problems. Therefore, in this investigation of inelastic buckling of long circular cylinders under compressive and torsional loads, an extension of Donnell's equations is considered.

The middle-surface strain variations and curvature changes that occur during buckling of a circular cylinder are related to the displacements as follows:

$$\left.\begin{aligned} \epsilon_1 &= \partial u/\partial x \\ \epsilon_2 &= (\partial v/R\,\partial\theta) + (w/R) \\ \epsilon_3 &= \frac{1}{2}\left(\frac{\partial u}{R\,\partial\theta} + \frac{\partial v}{\partial x}\right) \\ \chi_1 &= \partial^2 w/\partial x^2 \\ \chi_2 &= \partial^2 w/R^2\partial\theta^2 \\ \chi_3 &= \partial^2 w/R\,\partial x\,\partial\theta \end{aligned}\right\} \tag{B1}$$

The following simplified equilibrium equations as derived by Donnell (ref. 13) neglect certain terms which are of small magnitude when the circular cross section of the cylinder is distorted during buckling. In cases in which the cross section retains its circular shape during buckling the neglected terms are generally of some importance.

$$\Sigma F_x = \frac{\partial N_x'}{\partial x} + \frac{\partial N_{xy}'}{R\,\partial\theta} = 0 \tag{B2}$$

$$\Sigma F_\theta = \frac{\partial N_y'}{R\,\partial\theta} + \frac{\partial N_{xy}'}{\partial x} = 0 \tag{B3}$$

$$\Sigma F_z = -\frac{\partial^2 M_x'}{\partial x^2} - 2\frac{\partial^2 M_{xy}'}{R\,\partial x\,\partial\theta} - \frac{\partial^2 M_y'}{R^2\partial\theta^2} + \frac{N_y'}{R} + N_x\frac{\partial^2 w}{\partial x^2} + 2N_{xy}\frac{\partial^2 w}{R\,\partial x\,\partial\theta} +$$

$$N_y\frac{\partial^2 w}{R^2\partial\theta^2} + p = 0 \qquad \text{(B4)}$$

In equation (B4), N_x, N_{xy}, N_y, and p are prescribed external loadings, with N_x and N_y positive in compression. The terms containing a prime are the variations associated with buckling.

Inelastic Buckling

In appendix A, it was indicated that use of the no-strain-reversal model for inelastic buckling poses the difficulty that the external load must increase slightly during the buckling process. This is at variance with classical stability concepts which require the external load to remain constant during buckling. Therefore, some justification is necessary in order to use equilibrium equations based on constant external loads for inelastic buckling problems in which the external load must increase slightly. An attempt has been made to clarify this point which has been overlooked by previous investigators.

It is assumed that, in the inelastic-buckling process, the external loads increase slightly. Denoting this increment by δN, the external loads are increased as follows: $N_x + \delta N_x$, $N_{xy} + \delta N_{xy}$, $N_y + \delta N_y$, and $p + \delta p$. The terms containing a prime in equations (B2) to (B4) are the middle-surface force and bending-moment variations arising from bending and twisting of the plate at buckling. Therefore, the slight increase in external load represented by δN can have only a negligible influence upon the primed terms in equations (B2) to (B4).

In equation (B4), the external loads N_x, N_{xy}, N_y, and p appear. If these loads are replaced by $N_x + \delta N_x$, . . ., $p + \delta p$, then terms such as $\delta N_x\left(\partial^2 w/\partial x^2\right)$ and δp appear which are clearly of higher order than those terms appearing in equation (B4) and can be neglected. Thus, it appears permissible to conclude that the slight increase in load required for the plate to remain inelastic during buckling is compatible with the use of equilibrium equations based on classical stability concepts.

Equilibrium Equations

By use of the force and moment variations (eqs. (A7) to (A12)) and the strain-displacement relations (eqs. (B1)) the equilibrium relations (eqs. (B2) to (B4)) can be written in terms of the displacements u, v, and w and their derivatives:

$$A_1 \frac{\partial^2 u}{\partial x^2} - \frac{A_{13}}{2} \frac{\partial^2 u}{R\,\partial x\,\partial\theta} + \frac{A_3}{4} \frac{\partial^2 u}{R^2 \partial\theta^2} - \frac{A_{13}}{4} \frac{\partial^2 v}{\partial x^2} + \left(\frac{A_{12}}{2} + \frac{A_3}{4}\right) \frac{\partial^2 v}{R\,\partial x\,\partial\theta} -$$

$$\frac{A_{23}}{4} \frac{\partial^2 v}{R^2 \partial\theta^2} + \frac{A_{12}}{2} \frac{\partial w}{R\,\partial x} - \frac{A_{23}}{4} \frac{\partial w}{R^2 \partial\theta} = 0 \tag{B5}$$

$$A_2 \frac{\partial^2 v}{R^2 \partial\theta^2} - \frac{A_{23}}{2} \frac{\partial^2 v}{R\,\partial x\,\partial\theta} + \frac{A_3}{4} \frac{\partial^2 v}{\partial x^2} - \frac{A_{13}}{4} \frac{\partial^2 u}{\partial x^2} + \left(\frac{A_{12}}{2} + \frac{A_3}{4}\right) \frac{\partial^2 u}{R\,\partial x\,\partial\theta} -$$

$$\frac{A_{23}}{4} \frac{\partial^2 u}{R^2 \partial\theta^2} + A_2 \frac{\partial w}{R^2 \partial\theta} - \frac{A_{23}}{4} \frac{\partial w}{R\,\partial x} = 0 \tag{B6}$$

$$D\left[A_1 \frac{\partial^4 w}{\partial x^4} - A_{13} \frac{\partial^4 w}{R\,\partial x^3 \partial\theta} + \left(A_{12} + A_3\right) \frac{\partial^4 w}{R^2 \partial x^2 \partial\theta^2} - A_{23} \frac{\partial^4 w}{R^3 \partial x\,\partial\theta^3} + \right.$$

$$\left. A_2 \frac{\partial^4 w}{R^4 \partial\theta^4}\right] + \frac{B}{R}\left(\frac{A_{12}}{2} \frac{\partial u}{\partial x} - \frac{A_{23}}{4} \frac{\partial u}{R\,\partial\theta} - \frac{A_{23}}{4} \frac{\partial v}{\partial x} + A_2 \frac{\partial v}{R\,\partial\theta} + A_2 \frac{w}{R}\right) +$$

$$N_x \frac{\partial^2 w}{\partial x^2} + 2N_{xy} \frac{\partial^2 w}{R\,\partial x\,\partial\theta} + N_y \frac{\partial^2 w}{R^2 \partial\theta^2} + p = 0 \tag{B7}$$

Equations (B5) to (B7) constitute a basic set of equilibrium differential equations for plastic buckling of circular cylinders. In the elastic case, $A_1 = A_2 = A_3 = A_{12} = 1$ and $A_{13} = A_{23} = 0$, and, by properly accounting for Poisson's ratio, equations (B5) to (B7) reduce to the following:

$$\frac{\partial^2 u}{\partial x^2} + \frac{1 - \nu_e}{2} \frac{\partial^2 u}{R^2 \partial \theta^2} + \frac{1 + \nu_e}{2} \frac{\partial^2 v}{R \, \partial x \, \partial \theta} + \frac{\nu_e}{R} \frac{\partial w}{\partial x} = 0 \tag{B8}$$

$$\frac{\partial^2 v}{R^2 \partial \theta^2} + \frac{1 - \nu_e}{2} \frac{\partial^2 v}{\partial x^2} + \frac{1 + \nu_e}{2} \frac{\partial^2 u}{R \, \partial x \, \partial \theta} + \frac{\partial w}{R^2 \partial \theta} = 0 \tag{B9}$$

$$D\nabla^4 w + \frac{B}{R}\left(\nu_e \frac{\partial u}{\partial x} + \frac{\partial v}{R \, \partial \theta} + \frac{w}{R}\right) + N_x \frac{\partial^2 w}{\partial x^2} + 2N_{xy} \frac{\partial^2 w}{R \, \partial x \, \partial \theta} + N_y \frac{\partial^2 w}{R^2 \partial \theta^2} + p = 0 \tag{B10}$$

By suitable manipulation of equations (B8) to (B10), the above set of equations can be reduced to a single equation in deflection w known as Donnell's equation:

$$D\nabla^8 w + \frac{Et}{R^2} \frac{\partial^4 w}{\partial x^4} + \nabla^4 \left(N_x \frac{\partial^2 w}{\partial x^2} + 2N_{xy} \frac{\partial^2 w}{R \, \partial x \, \partial \theta} + N_y \frac{\partial^2 w}{R^2 \partial \theta^2} + p\right) = 0 \tag{B11}$$

APPENDIX C

AXIAL COMPRESSIVE BUCKLING OF A LONG CYLINDER

For a long circular cylinder subjected to axial compression, $\sigma_y = \tau = 0$. The value of the term σ_i which appears in equations (A13) is given by equation (A1) as discussed in reference 5 and, therefore, for this case $\sigma_i = \sigma_x$. Thus, the plasticity coefficients reduce to

$$\left.\begin{aligned} A_1 &= \frac{1}{4} + \frac{3}{4}\frac{E_t}{E_s} \\ A_2 = A_3 &= A_{12} = 1 \\ A_{13} &= A_{23} = 0 \end{aligned}\right\} \tag{C1}$$

Consequently, equilibrium equations (B5) to (B7) reduce to the following equations:

$$A_1 \frac{\partial^2 u}{\partial x^2} + \frac{1}{4}\frac{\partial^2 u}{R^2 \partial \theta^2} + \frac{3}{4}\frac{\partial^2 v}{R\,\partial x\,\partial \theta} + \frac{1}{2}\frac{\partial w}{R\,\partial x} = 0 \tag{C2}$$

$$\frac{\partial^2 v}{R^2 \partial \theta^2} + \frac{1}{4}\frac{\partial^2 v}{\partial x^2} + \frac{3}{4}\frac{\partial^2 u}{R\,\partial x\,\partial \theta} + \frac{\partial w}{R^2 \partial \theta} = 0 \tag{C3}$$

$$D\left(A_1 \frac{\partial^4 w}{\partial x^4} + 2\frac{\partial^4 w}{R^2 \partial x^2 \partial \theta^2} + \frac{\partial^4 w}{R^4 \partial \theta^4}\right) + \frac{B}{R}\left(\frac{1}{2}\frac{\partial u}{\partial x} + \frac{\partial v}{R\,\partial \theta} + \frac{w}{R}\right) + N_x \frac{\partial^2 w}{\partial x^2} = 0 \tag{C4}$$

Compressive tests of cylinders which buckle plastically indicate that an axisymmetric form of buckling often occurs. Therefore, if this mode of instability is assumed, the displacements are independent of the θ coordinate and all derivatives containing θ vanish. Thus, equations (C2) to (C4) reduce to the following forms:

$$A_1 \frac{\partial^2 u}{\partial x^2} + \frac{1}{2} \frac{\partial w}{R \partial x} = 0 \tag{C5}$$

$$\frac{\partial^2 v}{\partial x^2} = 0 \tag{C6}$$

$$DA_1 \frac{\partial^4 w}{\partial x^4} + \frac{B}{R}\left(\frac{1}{2} \frac{\partial u}{\partial x} + \frac{w}{R}\right) + N_x \frac{\partial^2 w}{\partial x^2} = 0 \tag{C7}$$

By performing the operation $\partial/\partial x$ on equation (C7) and then using equation (C5), a single equilibrium equation in w is obtained:

$$DA_1 \frac{\partial^5 w}{\partial x^5} + \frac{B}{R^2}\left(1 - \frac{1}{4A_1}\right)\frac{\partial w}{\partial x} + N_x \frac{\partial^3 w}{\partial x^3} = 0 \tag{C8}$$

A solution to equation (C8) can be written in the following form:

$$w = w_m \sin(\pi x/\lambda) \tag{C9}$$

where

$$\lambda = l/m$$

Upon substituting the appropriate derivatives of equation (C9) into equation (C8) and using the definitions of D, B, and A_1 given by equations (A15), (A14), and (C1), respectively, and the relation $N_x = \sigma_{cr} t$, the following nontrivial solution is obtained:

$$\sigma_{cr} = \frac{E_s t^2}{9}\left(\frac{1}{4} + \frac{3}{4}\frac{E_t}{E_s}\right)\frac{\pi^2}{\lambda^2} + \frac{E_t}{R^2\left(\frac{1}{4} + \frac{3}{4}\frac{E_t}{E_s}\right)}\frac{\lambda^2}{\pi^2} \tag{C10}$$

The cylinder is considered to be long, so that many waves form along the length and therefore σ_{cr} can be considered as a continuous function of λ. By minimizing equation (C10) with respect to the wave length,

$$\sigma_{cr} = \frac{2}{3} E_s \frac{t}{R}\left(\frac{E_t}{E_s}\right)^{1/2} \tag{C11}$$

The corresponding half wave length of the buckles

$$\lambda = \pi\left(\frac{1}{4} + \frac{3}{4}\frac{E_t}{E_s}\right)^{1/2}\left(\frac{Rt}{3}\right)^{1/2}\left(\frac{E_s}{E_t}\right)^{1/4} \tag{C12}$$

For the elastic case, the corresponding solutions are:

$$\sigma_{cr} = \left[3\left(1 - \nu_e^2\right)\right]^{-1/2} E \frac{t}{R} \tag{C13}$$

$$\lambda = \pi(Rt)^{1/2}\left[12\left(1 - \nu_e^2\right)\right]^{-1/4} \tag{C14}$$

By comparing the coefficients which appear in equations (C11) and (C13), it can be observed that the coefficient in equation (C11) can be obtained by substituting a value of 1/2 for ν_e in equation (C13). Thus, the following relations can be written which are exact in the elastic and fully plastic ranges and result in an excellent degree of approximation in the inelastic range:

$$\sigma_{cr} = \left[3\left(1 - \nu^2\right)\right]^{-1/2} E_s\left(E_t/E_s\right)^{1/2} \frac{t}{R} \tag{C15}$$

$$\lambda = \pi\left(\frac{1}{4} + \frac{3}{4}\frac{E_t}{E_s}\right)^{1/2}\left(\frac{E_s}{E_t}\right)^{1/4}(Rt)^{1/2}\left[12\left(1 - \nu^2\right)\right]^{-1/4} \tag{C16}$$

APPENDIX D

TORSIONAL BUCKLING OF A LONG CYLINDER

For a long circular cylinder subjected to torsional moments at the ends, $\sigma_x = \sigma_y = 0$. The value of σ_i which appears in equations (A13) is given by equation (A1). For this case,

$$\sigma_i = (3)^{1/2}\tau \tag{D1}$$

The plasticity coefficients reduce to

$$\left.\begin{aligned} A_1 = A_2 = A_{12} = 1 \\ A_{13} = A_{23} = 0 \end{aligned}\right\} \tag{D2}$$

$$A_3 = E_t/E_s \tag{D3}$$

Consequently, the equilibrium equations (eqs. (B5) to (B7)) reduce to the following expressions:

$$\frac{\partial^2 u}{\partial x^2} + \frac{A_3}{4}\frac{\partial^2 u}{R^2\partial\theta^2} + \frac{(2 + A_3)}{4}\frac{\partial^2 v}{R\,\partial x\,\partial\theta} + \frac{1}{2}\frac{\partial w}{R\,\partial x} = 0 \tag{D4}$$

$$\frac{\partial^2 v}{R^2\partial\theta^2} + \frac{A_3}{4}\frac{\partial^2 v}{\partial x^2} + \frac{(2 + A_3)}{4}\frac{\partial^2 u}{R\,\partial x\,\partial\theta} + \frac{\partial w}{R\,\partial\theta} = 0 \tag{D5}$$

$$D\left[\frac{\partial^4 w}{\partial x^4} + (1 + A_3)\frac{\partial^4 w}{R^2\partial x^2\partial\theta^2} + \frac{\partial^4 w}{R^4\partial\theta^4}\right] + \frac{B}{R}\left(\frac{1}{2}\frac{\partial u}{\partial x} + \frac{\partial v}{R\,\partial\theta} + \frac{w}{R}\right) +$$

$$2N_{xy}\frac{\partial^2 w}{R\,\partial x\,\partial\theta} = 0 \tag{D6}$$

By multiplying equation (D6) by R^2/B and letting

$$\left.\begin{aligned} \beta &= \frac{D}{BR^2} = \frac{t^2}{12R^2} \\ \varphi &= \frac{N_{xy}}{B} = \frac{\tau_{cr}}{(4/3)E_s} \end{aligned}\right\} \tag{D7}$$

Equation (D6) can be reduced to the more convenient form:

$$\beta\left[R^4 \frac{\partial^4 w}{\partial x^4} + \left(1 + A_3\right)R^2 \frac{\partial^4 w}{\partial x^2 \partial \theta^2} + \frac{\partial^4 w}{\partial \theta^4}\right] + \frac{R}{2}\frac{\partial u}{\partial x} + \frac{\partial v}{\partial \theta} + w + 2\varphi R \frac{\partial^2 w}{\partial x\, \partial \theta} = 0 \tag{D8}$$

Following the method of solution for torsional elastic buckling of a cylinder as given by Timoshenko (ref. 1), the following relations are used for the displacements:

$$\left.\begin{aligned} u &= u_{mn} \cos\left(\frac{\lambda x}{R} - n\theta\right) \\ v &= v_{mn} \cos\left(\frac{\lambda x}{R} - n\theta\right) \\ w &= w_{mn} \sin\left(\frac{\lambda x}{R} - n\theta\right) \end{aligned}\right\} \tag{D9}$$

The angle which the helical buckle makes with the original generator of the cylinder is given by

$$\tan \omega = \lambda/n \tag{D10}$$

Since the cylinder is assumed to be long, the boundary conditions at the ends are relatively unimportant and, therefore, equations (D9) can be used although they do not satisfy the usual boundary conditions of simple support or clamping.

The substitution of the appropriate derivatives of equations (D9) into equations (D4), (D5), and (D8) results in the following matrix equation:

$$\begin{vmatrix} -\left(\lambda^2 + \frac{A_3}{4} n^2\right) & \frac{\left(2 + A_3\right)}{4} \lambda n & \frac{1}{2} \lambda \\ \left(\frac{2 + A_3}{4}\right) \lambda n & -\left(n^2 + \frac{A_3}{4} \lambda^2\right) & -n \\ \frac{1}{2} \lambda & -n & -\left[1 + 2\varphi\lambda n + \beta\lambda^4 + 2\beta\left(1 + A_3\right)\lambda^2 n^2 + \beta n^4\right] \end{vmatrix} \begin{Vmatrix} u_{mn} \\ v_{mn} \\ w_{mn} \end{Vmatrix} = 0 \qquad \text{(D10)}$$

A nontrivial solution requires the determinant to vanish independently. Upon expanding the determinant, the following result is obtained:

$$\varphi = \frac{\frac{3A_3}{4} \lambda^4 + \beta\left[n^4 + \left(1 + A_3\right)\lambda^2 n^2 + \lambda^4\right]\left[A_3 n^4 + \left(3 - A_3\right)\lambda^2 n^2 + A_3 \lambda^4\right]}{2\lambda n\left[A_3 n^4 + \left(3 - A_3\right)\lambda^2 n^2 + A_3 \lambda^4\right]} \qquad \text{(D11)}$$

As in the elastic case, very small values of λ yield the smallest value of φ. Furthermore, by assuming β to be small, equation (D11) simplifies to

$$\varphi = \frac{(3/4)\lambda^4 + \beta n^8}{2\lambda n^5} \qquad \text{(D12)}$$

Note that the term A_3 cancels out of equation (D12) under these assumptions and, therefore, the solution for φ is independent of the value of A_3 given by equation (D3).

For a long cylinder a minimum value of φ is obtained for $n = 2$ which corresponds to the familiar two-lobe buckling. Therefore, equation (D12) becomes

$$\varphi = \frac{(3/4)\lambda^4 + 256\beta}{64\lambda} \qquad \text{(D13)}$$

By differentiating with respect to λ,

$$\lambda = 4\left(\frac{2}{3}\right)^{1/2}\beta^{1/4}$$

$$= \frac{4}{3}\left(3t^2/R^2\right)^{1/4} \tag{D14}$$

Upon substituting equation (D14) into equation (D13) and simplifying,

$$\varphi = \frac{4}{3}\left(\frac{3}{2}\right)^{1/2}\beta^{3/4} \tag{D15}$$

By use of equations (D7)

$$\tau_{cr} = \frac{4}{9}(3)^{-1/4}E_s(t/R)^{3/2}$$

$$= 0.338E_s(t/R)^{3/2} \tag{D16}$$

The corresponding elastic solution can be obtained by substituting $1 - \nu_e^2$ for the coefficient $3/4$ in equations (D13) and (D7):

$$\tau_{cr} = \left[\left(\frac{3}{2}\right)(6)^{1/2}\right]^{-1}\left(1 - \nu_e^2\right)^{-3/4}E(t/R)^{3/2}$$

$$= 0.272\left(1 - \nu_e^2\right)^{-3/4}E(t/R)^{3/2} \tag{D17}$$

$$\lambda = \left[2\left(1 - \nu_e^2\right)^{-1/2}t/R\right]^{1/2} \tag{D18}$$

By identifying the coefficient $4/3$ which appears in equations (D13) and (D7) as the limiting value of $\left(1 - \nu^2\right)^{-1}$ with $\nu = 1/2$, it is then possible to combine equation (D16) with (D17) and equation (D14) with (D18):

$$\tau_{cr} = 0.272\left(1 - \nu^2\right)^{-3/4} E_s (t/R)^{3/2} \tag{D19}$$

$$\lambda = \left[2\left(1 - \nu^2\right)^{-1/2} t/R\right]^{1/2} \tag{D20}$$

Equations (D19) and (D20) are exact for the elastic and plastic ranges and constitute excellent approximations in the inelastic range.

REFERENCES

1. Timoshenko, S.: Theory of Elastic Stability. First ed., McGraw-Hill Book Co., Inc., 1936.

2. Bijlaard, P. P.: Theory and Tests on the Plastic Stability of Plates and Shells. Jour. Aero. Sci., vol. 16, no. 9, Sept. 1949, pp. 529-541.

3. Ilyushin, A. A.: The Elasto-Plastic Stability of Plates. NACA TM 1188, 1947.

4. Handelman, G. H., and Prager, W.: Plastic Stability of a Rectangular Plate Under Edge Thrusts. NACA Rep. 946, 1949. (Supersedes NACA TN 1530.)

5. Stowell, Elbridge Z.: A Unified Theory of Plastic Buckling of Columns and Plates. NACA Rep. 898, 1948. (Supersedes NACA TN 1556.)

6. Stowell, Elbridge Z.: Critical Shear Stress of an Infinitely Long Plate in the Plastic Region. NACA TN 1681, 1948.

7. Gerard, George: Secant Modulus Method for Determining Plate Instability Above the Proportional Limit. Jour. Aero. Sci., vol. 13, no. 1, Jan. 1946, pp. 38-44, 48.

8. Stowell, Elbridge Z.: Compressive Strength of Flanges. NACA Rep. 1029, 1951. (Supersedes NACA TN 2020.)

9. Pride, Richard A., and Heimerl, George J.: Plastic Buckling of Simply Supported Compressed Plates. NACA TN 1817, 1949.

10. Peters, Roger W.: Buckling of Long Square Tubes in Combined Compression and Torsion and Comparison With Flat-Plate Buckling Theories. NACA TN 3184, 1954.

11. Gerard, George: Critical Shear Stress of Plates Above the Proportional Limit. Jour. Appl. Mech., vol. 15, no. 1, Mar. 1948, pp. 7-12.

12. Bijlaard, P. P.: On the Plastic Stability of Thin Plates and Shells. Verh. Koninklijke Nederlandsche Akademie van Wetenschappen, vol. L, no. 7, Sept. 1947, pp. 765-775.

13. Donnell, L. H.: Stability of Thin-Walled Tubes Under Torsion. NACA Rep. 479, 1933.

14. Osgood, William R.: The Crinkling Strength and the Bending Strength of Round Aircraft Tubing. NACA Rep. 632, 1938.

15. Moore, R. L., and Holt, Marshall: Beam and Torsion Tests of Aluminum-Alloy 61S-T Tubing. NACA TN 867, 1942.

16. Anon.: Strength of Metal Aircraft Elements. ANC-5, Munitions Board Aircraft Committee, Revised ed., June 1951.

17. Gerard, George, and Wildhorn, Sorrel: A Study of Poisson's Ratio in the Yield Region. NACA TN 2561, 1952.

18. Batdorf, S. B.: A Simplified Method of Elastic-Stability Analysis for Thin Cylindrical Shells. I - Donnell's Equation. NACA TN 1341, 1947.

19. Stang, Ambrose H., Ramberg, Walter, and Back, Goldie: Torsion Tests of Tubes. NACA Rep. 601, 1937.

20. Moore, R. L., and Paul, D. A.: Torsional Stability of Aluminum Alloy Seamless Tubing. NACA TN 696, 1939.

21. Tsien, Hsue-Shen: A Theory for the Buckling of Thin Shells. Jour. Aero. Sci., vol. 9, no. 10, Aug. 1942, pp. 373-384.

22. Donnell, L. H., and Wan, C. C.: Effect of Imperfections on Buckling of Thin Cylinders and Columns Under Axial Compression. Jour. Appl. Mech., vol. 17, no. 1, Mar. 1950, pp. 73-83.

TABLE 1

TEST DATA ON COMPRESSIVE STRENGTH OF TUBES

(a) 2017-T4 aluminum-alloy data of reference 14

d/t	σ_f, ksi	η_c
98.4	41.8	0.330
97.9	41.9	.327
79.2	45.2	.288
78.4	45.6	.287
78.1	43.6	.273
63.7	47.0	.241
63.7	47.4	.242
62.2	46.3	.230
61.5	46.0	.226
61.5	46.2	.228
61.4	46.0	.226

(b) 6061-T6 aluminum-alloy data of reference 15

d, in.	t, in.	σ_f, ksi	η_c
1.32	0.016	40.8	0.281
	.023	39.0	.187
	.033	41.9	.140
	.066	46.3	.077
	.132	52.7	.044
2.00	0.025	38.6	0.257
	.033	40.8	.206
	.050	43.6	.146
	.100	43.6	.073
	.200	53.3	.044

TABLE 2

TEST DATA ON TORSIONAL STRENGTH OF LONG TUBES FROM REFERENCE 19

(a) 2017-T4 aluminum-alloy tubes

l/d	t/d	τ_f, ksi	η_s
19.9	0.02235	23.1	0.792
19.9	.02516	23.4	.698
60.0	.02848	24.2	.580
19.9	.03231	24.9	.491
59.8	.03242	26.0	.513
39.9	.02195	22.8	.830
13.3	.02903	25.1	.596
39.9	.02896	24.1	.572
13.3	.03273	26.4	.512
40.0	.03312	26.1	.506
30.0	.03350	25.7	.491

(b) Chrome-molybdenum tubes

l/d	t/d	τ_{yield}, ksi	τ_f, ksi	η_s
25.3	0.04055	48.6	50.6	0.262
25.3	.04040	47.9	50.4	.261
79.9	.04020	49.5	51.1	.264
30.1	.02330	47.2	43.8	.530
12.6	.03486	49.8	47.4	.309

TABLE 3

TEST DATA ON TORSIONAL STRENGTH OF TUBES

(a) 6051-T6 aluminum-alloy tubes of moderate length from reference 20

l/d	d/t = 77		d/t = 104		d/t = 139	
	τ_f, ksi	η_s	τ_f, ksi	η_s	τ_f, ksi	η_s
1	21.6	0.412	18.9	0.525	18.4	0.728
1	21.9	.418	19.5	.542	18.4	.728
2	21.4	.580	18.8	.740	17.0	.950
2	21.9	.594	19.7	.765	16.5	.923
4	21.2	.810	17.7	.984	12.6	1.00
4	21.3	.814	18.6	1.03	12.4	.982
8	20.1	1.09	13.9	1.09	9.2	1.035
8	19.2	1.04	14.0	1.10	9.2	1.035
16	13.5	1.03	9.8	1.09	6.5	1.02
16	12.5	.957	9.6	1.08	6.5	1.02

(b) 6061-T6 aluminum-alloy tubes from reference 15

Length (a)	d/t	l/d	τ_f, ksi	η_s
M	80.6	5.7	19.1	0.816
M	80.6	17.0	10.4	.813
L	80.6	27.6	9.3	.795
M	80.6	11.5	15.4	.987
M	58.8	5.7	18.6	.543
L	58.8	17.0	17.4	.927
L	58.8	27.6	15.2	.810
M	39.4	5.7	22.7	.403
L	39.4	17.0	22.3	.648
L	39.4	27.6	22.0	.640
M	60.6	11.5	20.2	.928

[a]M, moderate length; L, long.

TABLE 4

SUMMARY OF DATA USED FOR CORRELATION

Material	Loading	Figure	η	Stress-strain data	Remarks
2017-T4	Compression	1	Eq. (4)	Compression	Excellent agreement; limited test data
6061-T6	Compression	1	Eq. (4)	[a] σ_{cy}	Fair agreement; limited test data
2017-T4	Torsion	2	Eq. (17)	Shear	Excellent agreement; wide range of test data
Chrome-molybdenum	Torsion	2	Eq. (17)	Shear	Theory high; limited test data
6051-T6	Torsion	3	Eq. (10)	Tension	Fair agreement; moderate length tubes
6061-T6	Torsion	3	Eq. (10)	[a] σ_y	Good agreement; moderate and long tubes

[a]Tensile and compressive yield stress given. Stress-strain data obtained from ref. 16 for these yield values.

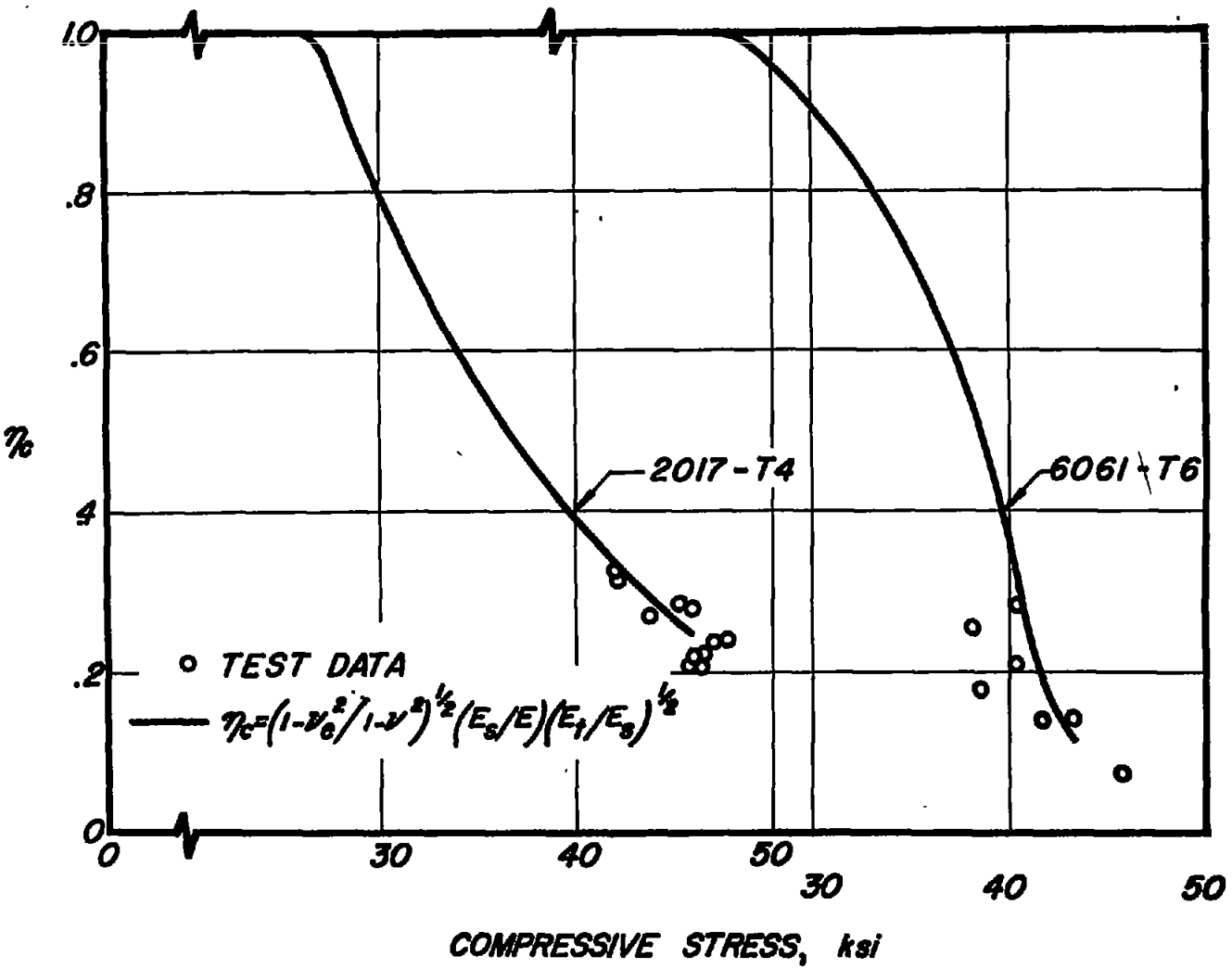

Figure 1.- Plasticity-reduction factors for compressive buckling of aluminum-alloy tubes.

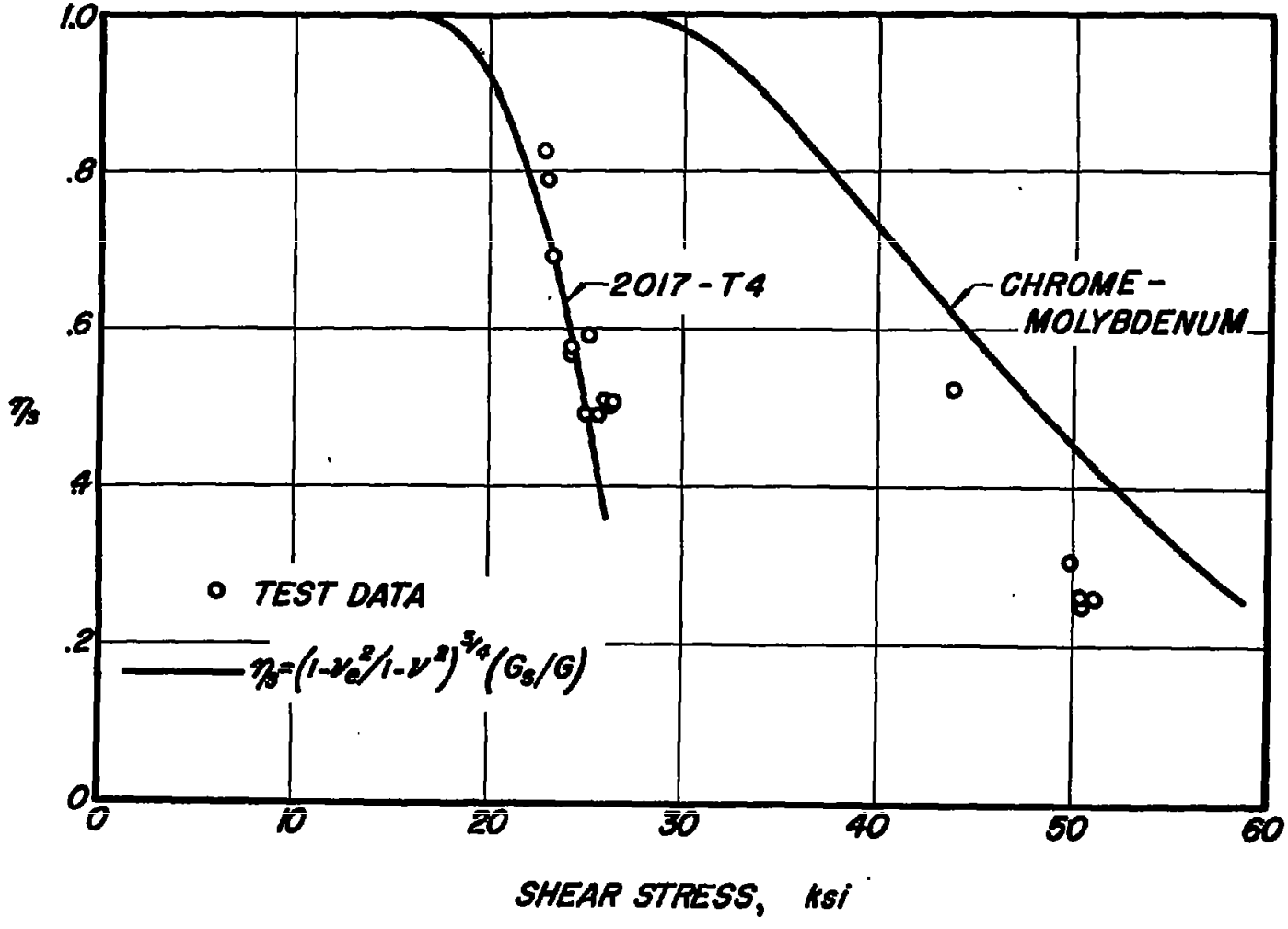

Figure 2.- Plasticity-reduction factors for torsional buckling of long tubes.

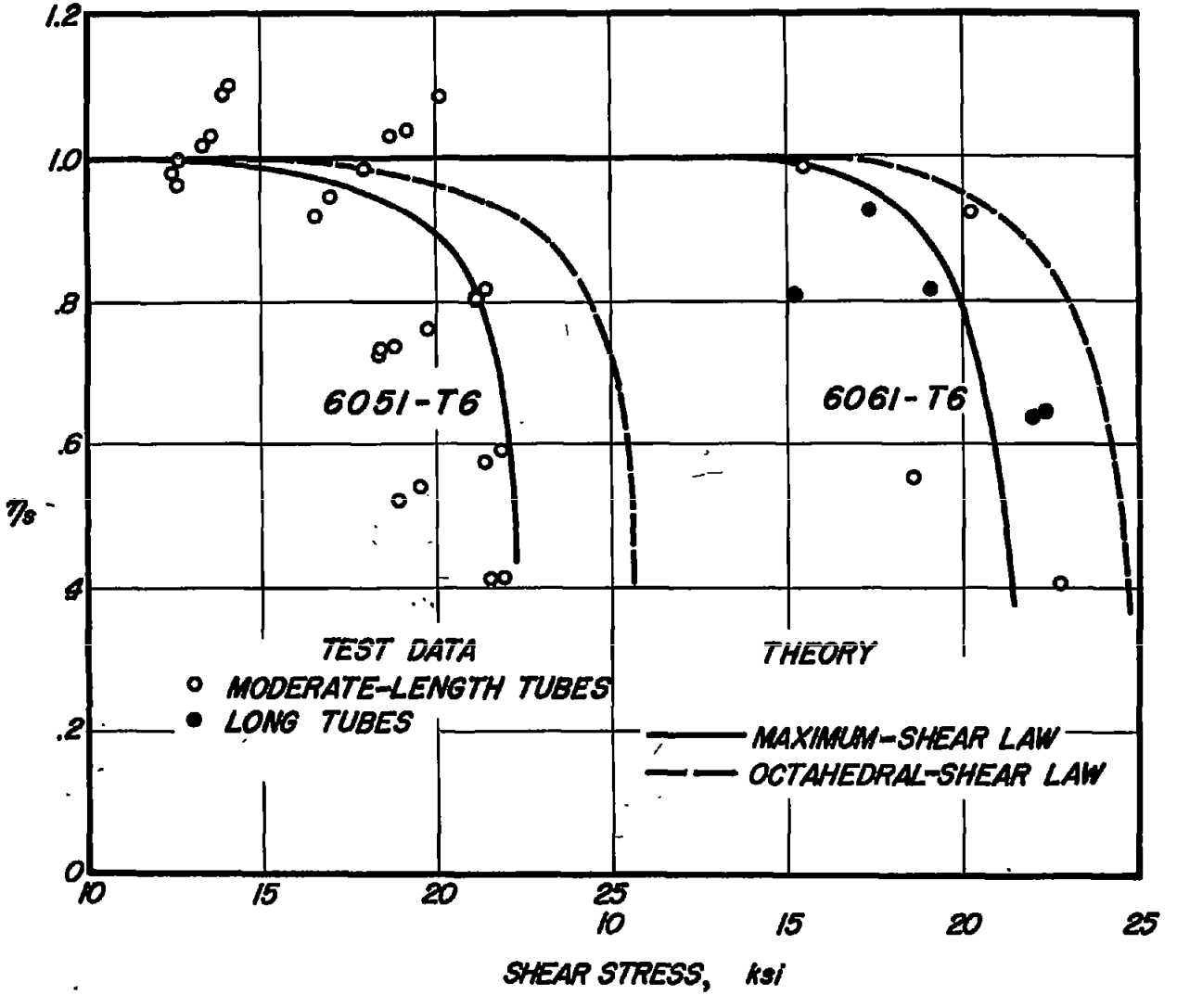

Figure 3.- Plasticity-reduction factors for torsional buckling of tubes.

$$\eta_s = (1 - \nu_e^2/1 - \nu^2)^{3/4}(E_s/E).$$